REVIEW   **Open Access**

Tumor extracellular matrix: lessons from the second-harmonic generation microscopy

Rodrigo de Andrade Natal[1*] ![ORCID], Javier Adur[2], Carlos Lenz Cesar[3,4] and José Vassallo[1,5]

Abstract

Extracellular matrix (ECM) represents more than a mere intercellular cement. It is physiologically active in cell communication, adhesion and proliferation. Collagen is the most abundant protein, making up to 90% of ECM, and 30% of total protein weight in humans. Second-harmonic generation (SHG) microscopy represents an important tool to study collagen organization of ECM in freshly unfixed tissues and paraffin-embedded tissue samples. This manuscript aims to review some of the applications of SHG microscopy in Oncologic Pathology, mainly in the study of ECM of epithelial tumors. It is shown how collagen parameters measured by this technique can aid in the differential diagnosis and in prognostic stratification. There is a tendency to associate higher amount, lower organization and higher linearity of collagen fibers with tumor progression and metastasizing. These represent complex processes, in which matrix remodeling plays a central role, together with cancer cell genetic modifications. Integration of studies on cancer cell biology and ECM are highly advantageous to give us a more complete picture of these processes. As microscopic techniques provide topographic information allied with biologic characteristics of tissue components, they represent important tools for a more complete understanding of cancer progression. In this context, SHG has provided significant insights in human tumor specimens, readily available for Pathologists.

Keywords: Second-harmonic generation microscopy, Collagen, Tumor extracellular matrix, Tumor microenvironment, Oncologic pathology

Introduction

Non-cellular components of tissue, or extracellular matrix (ECM), provide biochemical and biomechanical support for cellular constituents. More than a mere intercellular cement, ECM is physiologically active in cell communication, adhesion and proliferation (Frantz et al. 2010). It is composed of approximately 300 proteins, the proportion between which gives the precise composition to specific structures (Naba et al. 2012). Fibrous proteins, such as collagen, elastin, fibronectins and laminins, are the major constituents of the ECM, which, together with proteoglycans, that are locally secreted and

assembled, form the structural framework of most tissues (Frantz et al. 2010). Among the fibrous proteins, collagen is the most abundant in ECM, making up to 90% of ECM and 30% of total protein weight in humans (van der Rest and Garrone 1991).

Molecular approaches have highlighted genes that encode ECM components, which have been correlated with tumor behavior and clinical outcomes (Finak et al. 2008; Ramaswamy et al. 2003). Increased expression of genes encoding proteins that mediate extracellular remodeling has been associated with increased mortality in patients with breast, lung and gastric cancer. Such studies corroborate histological findings that show association between excessive ECM deposition and worse prognosis in solid tumors (Chang et al. 2005; Chang et al. 2004). Further, increased collagen deposition is the

* Correspondence: rodrigo.natal.med@gmail.com
[1]Laboratory of Investigative and Molecular Pathology, Faculty of Medical Sciences, University of Campinas. Rua Tessália Vieira de Camargo, 126, Zip code: 13083-970, Campinas, São Paulo, Brazil
Full list of author information is available at the end of the article

most well recognized ECM alteration that occurs inside the tumor tissue (Hasebe et al. 1997; Colpaert et al. 2003; Huijbers et al. 2010; Kauppila et al. 1998; Zhu et al. 1995; Gould et al. 1990; Boyd et al. 2002).

In the context of cancer biology, collagen regulates the biophysical and biochemical properties of tumor microenvironment (TME), which modulate cancer cell polarity, migration and signaling (Fraley et al. 2012; 2010; Levental et al. 2009a; Paszek et al. 2005; van Kempen et al. 2003). Thus, careful evaluation of ECM collagen could provide important information about the tumor.

The purpose of the present review is to discuss the role of a significant tool to characterize collagen in TME, by second-harmonic generation (SHG) microscopy, presenting some of the experience gained in Oncologic Pathology.

Multiphoton microscopy and second-harmonic generation microscopy

Multiphoton microscopy, a form of laser-scanning microscopy, utilizes nonlinear excitation to generate signal only within a thin raster-scanned plane (Tajik 2018). Its applications are diverse, as this device has become a choice for fluorescence microscopy, mainly in thick tissues and live animals.

One of its most striking features is its intrinsically focal-plane selectivity, without need of any confocal optical tool (e.g., pinhole). It offers a modest resolution improvement over conventional microscopy at the same wavelength since the point of spread function is squared, besides improved penetration and reduced damage conferred by the longer excitation wavelength (Cox 2011).

However, although multiphoton microscopy offers many advantages compared to conventional microscopy, it also has limitations and drawbacks. One obvious limitation is still the high cost of the appropriate ultrafast laser.

A second limitation pertains to the accelerated photobleaching in some nonlinear optical microscopies, like two-photons excited fluorescence (TPEF). Although TPEF produces photobleaching only in the focal plane, within the focal volume, high order photobleaching is observed. Compared to confocal microscopy, where the photobleaching rate increases quasi linearly with the excitation power, in multiphoton microscopy, the higher photon density activates more photobleaching pathways, resulting in accelerated effect (Kalies et al. 2011; Patterson and Piston 2000), however this effect it not observed in other non-linear microscopies, such as SHG.

Finally, specific limitations arise if the multiphoton laser beam interacts linearly with chromophores in the sample. For example, near infrared light is absorbed by the photosynthetic complex; other naturally occurring chromophores, such as the pigment melanin, can limit

tissue imaging by causing thermal and mechanical damage in an experiment (Ustione and Piston 2011).

TPEF, SHG (Campagnola et al. 2002; 2001; Dombeck et al. 2003; Freund and Deutsch 1986) and third-harmonic generation (THG) (Müller et al. 1998) are examples of multiphoton microscopy and can also be used for specific imaging. SHG was one of the earliest forms of biological nonlinear microscopy proposed (Sheppard and Kompfner 1978). Figure 1 demonstrates the physical representation of each process.

The SHG microscope has been successfully integrated into biological research. Therefore, in the past two decades, as femtosecond laser sources have become more robust and commercially available, publications related to this application have grown exponentially (Fig. 2). In biological and medical sciences, the role of SHG has been used in high-resolution optical microscopes. SHG imaging modality can probe molecular organization, symmetry, orientation, alignments and ultrastructures on the micro as well as the nanoscale. Because most biological structures are not highly ordered, they are optically isotropic and do not produce any SHG signal. Only those few biological structures that are ordered or that involve some spatial organizations that break the optical centro-symmetry can produce harmonic signal. Namely collagen, the major protein of the extracellular matrix, is one of the best-known SHG structures in biology. Collagen fibrils often aggregate into larger, cable-like bundles, several micrometers in diameter. This regularly staggered packing order provides the needed structural conditions for efficient SHG (Williams et al. 2005). An example of detailed schematic workstation setup has been previously shown (Natal et al. 2018a).
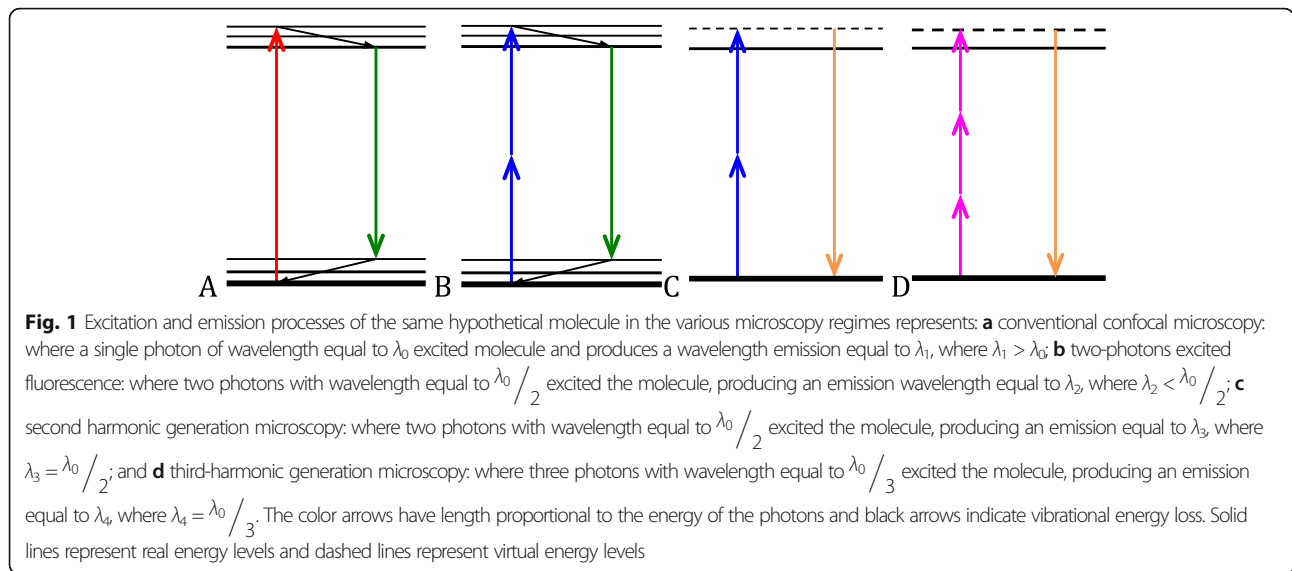
Second-harmonic generation microscopy in oncology pathology

Gynecological pathology

Breast cancer

In breast cancer was described three forms of collagen deposits in breast cancer, known as *tumor associated collagen signature* (TACS). In TACS-1, dense collagen was deposited in areas around the tumor, which was indicated by increased signal intensity, as hallmark for locating small tumor regions. In TACS-2, taut (straightened) collagen fibers were stretched around the tumor, indicating growth and increasing in tumor volume. Finally, in TACS-3, radially aligned collagen fibers can be identified, facilitating cell motility, and pointing to the invasive and metastatic growth potential of the tumor (Provenzano et al. 2006a) (Fig. 3). Additionally, tumor progression and the risk of metastases was directly associated to the increased density of collagen (Provenzano et al. 2008).
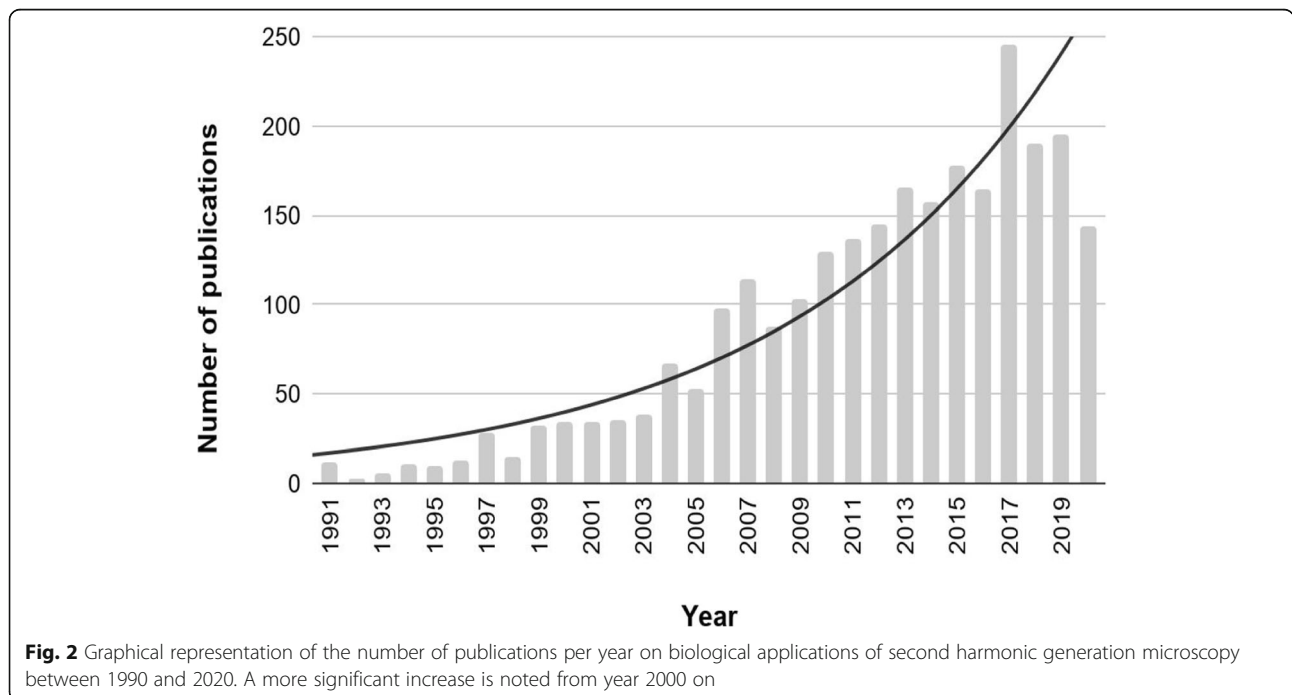
Considering the experimental findings in mice, TACS-3 phenotype facilitated tumor metastasis, a parameter

Fig. 1 Excitation and emission processes of the same hypothetical molecule in the various microscopy regimes represents: **a** conventional confocal microscopy: where a single photon of wavelength equal to λ_0 excited molecule and produces a wavelength emission equal to λ_1, where $\lambda_1 > \lambda_0$; **b** two-photons excited fluorescence: where two photons with wavelength equal to $\frac{\lambda_0}{2}$ excited the molecule, producing an emission wavelength equal to λ_2, where $\lambda_2 < \frac{\lambda_0}{2}$; **c** second harmonic generation microscopy: where two photons with wavelength equal to $\frac{\lambda_0}{2}$ excited the molecule, producing an emission equal to λ_3, where $\lambda_3 = \frac{\lambda_0}{2}$; and **d** third-harmonic generation microscopy: where three photons with wavelength equal to $\frac{\lambda_0}{3}$ excited the molecule, producing an emission equal to λ_4, where $\lambda_4 = \frac{\lambda_0}{3}$. The color arrows have length proportional to the energy of the photons and black arrows indicate vibrational energy loss. Solid lines represent real energy levels and dashed lines represent virtual energy levels

that could predict survival outcomes in human patients diagnosed with breast carcinoma. Patients diagnosed with invasive breast cancer with TACS-3 phenotype was associated with poor disease-specific and disease-free survival. This biomarker was also confirmed to be an independent prognostic indicator regardless of tumor grade, size, and estrogen receptor, progesterone receptor, or human epidermal growth factor receptor-2 (HER-2) immunohistochemical status. Surprisingly, TACS-3 was also prognostically independent of lymph node status (Conklin et al. 2011). It is noteworthy that in the model using mice, breast tumors were all of the luminal

molecular subtype (Hollern and Andrechek 2014). In addition, in women with the luminal subtype of invasive ductal carcinoma, higher deposition of collagen was associated with poorer prognosis (Natal et al. 2018b), (Fig. 4), including lymph node involvement (Kakkad et al. 2012).

Of note, changes in collagen quantity and organization were seen when areas of invasive ductal carcinoma were compared with areas of breast tissue without alterations (Natal et al. 2018b), as well as within the same areas along tumor progression (Brabrand et al. 2015). In addition, polarimetric SHG succeeded to reveal ultrastructural
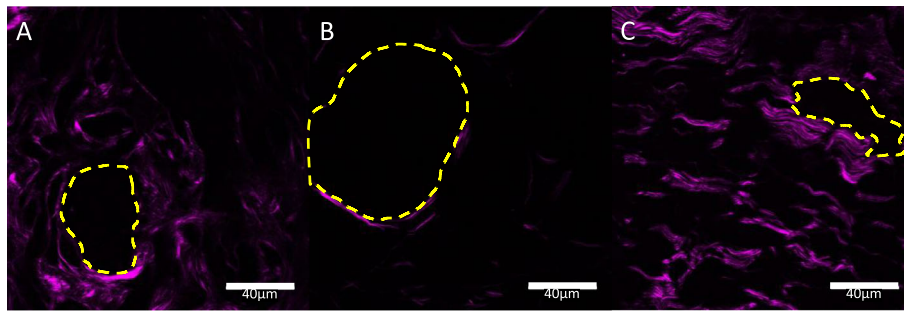

Fig. 2 Graphical representation of the number of publications per year on biological applications of second harmonic generation microscopy between 1990 and 2020. A more significant increase is noted from year 2000 on

Fig. 3 Second-harmonic generation images of breast cancer. Representation of *tumor associated collagen signatures* (TACS, see text): **a** TACS-1; **b** TACS-2; and **c** TACS-3

disorganization in the focal volume amongst the different molecular subtypes of breast carcinoma, therefore it could be used for the molecular classification (Golaraei et al. 2016).

In special types of invasive breast cancer, tubular carcinoma and invasive lobular carcinoma presented higher collagens fibers organization, generally these fibers are arranged parallel to the tumor invasion. Although, medullary, mucinous and papillary carcinomas showed an intense collagen fibers disorganization (Adur 2012; Natal et al. 2019).

Ductal carcinoma in situ and therapeutics agents also demonstrated changes in collagen parameters (Conklin et al. 2018) (Walsh et al. 2015; Wu et al. 2018). In ductal carcinoma in situ, radially deposition of collagen fibers was associated with a higher recurrence rate, while in chemotherapy, there was a disorganization of collagen fibers. Such changes may shed light in the mechanisms of tumor progression as well as of response to therapy (Bredfeldt et al. 2014).

In other breast lesions, fibroadenoma presented greater amounts of collagen than healthy breast tissue (Nie et al. 2015; Zheng et al. 2011) or phyllodes tumors (Tan et al. 2015). The difference in collagen deposition allowed distinction between these lesions with up to 71.4 and 84.4% sensitivity and specificity, respectively.

Ovary cancer
One of the earliest studies addressing ovarian cancer has demonstrated that neoplastic stroma diverged from healthy tissue. Women at high risk of developing ovarian cancer (i.e., BRCA1 or BRCA2 mutated) presented abnormal changes in the structure of ovarian collagen, similar to those found in neoplasia itself (Kirkpatrick et al. 2007).

Mathematical models applied to images satisfactorily distinguished healthy from neoplastic ovarian stroma (Tilbury et al. 2017; Wen et al. 2014). In this context, ovaries with malignancy could be characterized by lower cell density, denser collagen, as well as higher regularity

at both fibril and fiber levels (Nadiarnykh et al. 2010). Further, this method has been applied not only to differentiate adenomas from adenocarcinomas, but also for histological subtyping, such as to distinct serous from mucinous tumors (Adur et al. 2014; Adur et al. 2012; Campbell and Campagnola 2017; Zeitoune et al. 2017).

A study in mice has demonstrated that tumor evolution is marked by progressive alteration of collagen. Normal ovary showed very dense collagen at the surface, especially at what appeared to be the epithelial-stromal boundary. While collagen fibers at the surface were thin, linear and interweaved forming a tight-knit; stromal collagen, beyond these features, showed gaps (up to 400 μm for larger follicles) in areas with functional ovarian structures (e.g. follicles and corpora lutea). Atrophic ovary is quite similar, however the gaps were smaller, corresponding to small cysts. Tubular hyperplasia and granulosa cell tumor showed less collagen, former presented spaced far apart tangled appearance with clumps and latter presented revealed less tightly packed. Further, both cystic tumor and fibrosarcoma presented more linear to wavy collagen fibers, differentiating by slightly thicker collagen fibers and more spread out or tangled compared to normal ovary, respectively (Watson et al. 2014).

In addition to 2D images, 3D images can provide more details of collagen structure. This improvement allowed distinction between conditions, as normal from high risk ovarian stroma, benign from malignant tumors, low grade from high grade neoplasms, serous tumors from endometrioid tumors (Wen et al. 2016).

Gastrointestinal pathology
Upper gastrointestinal tract
Esophagus healthy submucosa was characterized by larger amounts of aligned collagen organized in large and spiral bundles. However, esophageal adenocarcinoma and esophageal squamous cell carcinoma submucosa was described by fine and distorted collagen fibers, with disorganized little collagen fibers (Chen et al. 2014; Xu et al. 2017).
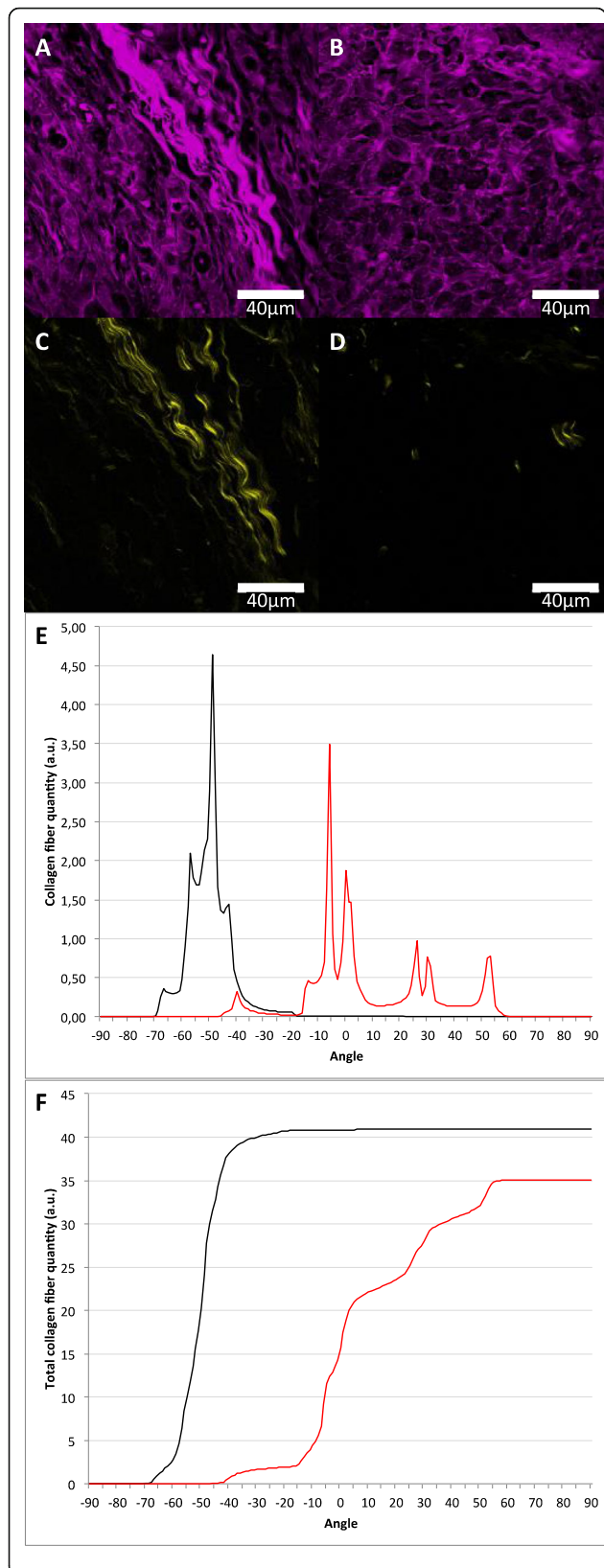
Fig. 4 Two cases of invasive ductal carcinoma of the breast. Images **a** and **c** show, respectively, two-photon-excited fluorescence microscopy (TPEF) and second harmonic generation (SHG) of a patient (P1) who presented disease progression (metastasis/recurrence). **b** and **d** show, respectively, TPEF and SHG of a patient (P2) whose disease did not progress. In graphs E and F, the black line corresponds to patient P1 and the red line to patient P2. Notice that in graph **e** collagen fibers are arranged between − 70° to − 20° (variation of 50°) for patient P1 and between − 50° to 60° (variation of 110°) for patient P2. In graph **f** it is shown that patient P1 had total amount of collagen fibers greater than patient P2. This is in line with previous evidence that intratumoral collagen with less angulation, that is, more organized, and that greater amounts of intratumoral collagen are associated with higher risk of disease progression

Of note, in Barrett's esophagus significant changes in collagen structure of the basal layer were found, with increased amount of collagen in the basement membrane, resulting in increased thickness (Mehravar et al. 2016). The progression of dysplasia severity was also associated to increase of basement membrane thickness (Mehravar et al. 2016).

In gastric cancer, collagen structure was evaluated according to the extent of invasion, and it was shown that cases with serosa infiltration by tumor were associated with reduction in amount and increase in disorganization of collagen fibers (Yan et al. 2016). Besides, higher values of collagen signature, based on parameters like quantity and alignment of collagen fibers, predicted early lymph node involvement (Chen et al. 2019).

Pancreas and liver

Chronic pancreatitis presented a variable collagen structure, with some ducts resembling normal ones, and others, with more abundant collagen, were similar to malignant ducts. In opposition, pancreatic ductal adenocarcinoma showed increased alignment, length, and width collagen around malignant ducts. Collagen fibers varied also with respect to tumor cellularity; fibers were sparsely deposited in highly cellular regions, whereas highly aligned collagen was seen in poor cellular areas. In addition, high alignment of collagen was associated with poor prognosis (Drifka et al. 2015). It was also observed a positive association between high collagen alignment and the increased expression of alpha-smooth muscle actin, which was related to poor prognosis (Drifka et al. 2016a, b).

In liver, the amount of collagen present in hepatocellular carcinomas (HCC) samples could distinguish well-differentiated tumors (histological grade I) from moderately to poorly differentiated tumors (histological grades II and III) (Lin et al. 2018). Histological grade I displayed low amounts of collagen fibers, which were scattered, in a slender strip, similar to the normal liver. In histological grade II, there was

an increase in the amount of collagen and the bundles became longer and thicker. In histological grade III there was an even greater increase in the amount of collagen and its deposition was heterogeneous throughout the tumor extension (Lin et al. 2018). Further, COL1A1 was significantly upregulated in HCC tumor tissues in comparison to normal tissues and conferred survival advantage and enhanced oncogenicity, promoting epithelial-to-mesenchymal transition (EMT) (Ma et al. 2019).

Colon and rectum
In colon, SHG imaging revealed different patterns in the outlines of basement membrane throughout normal-to-cancer progression. Normal mucosa presented a honeycomb arrangement of round-shaped regular basement membrane, with a concentrated collagen fiber in a submucosal layer, while precarcinomatous lesions revealed larger size and lower density of the tubular-shaped basement membrane. In cancer, basement membrane was missing (Maier et al. 2021; Xia et al. 2017; Zhuo et al. 2012) and collagen fibers of basement membrane were more disorganized and diminished, assuming varied directions as tumor invaded (Liu et al. 2013; Qiu et al. 2015).

In rectal cancer, cases with non-compromised surgical margins were characterized by collagen fibers around the glands, while in cases with positive surgical margins there was significant decrease or loss of such fibers (Yan et al. 2014). Besides, quantification of collagen structure has shown also potential of monitoring response to neoadjuvant chemotherapy in colorectal cancer, since the adequate response to therapy was accompanied by a greater deposition of collagen (Li et al. 2017).

Urogenital pathology
Deposition of higher amount and more linear collagen fibers throughout the tumor was associated with worse prognosis in invasive bladder cancer (Brooks et al. 2016) and higher histological grade in renal cell carcinoma (Best et al. 2019).

Prostate cancer, in opposition to prostate benign lesions, showed change in collagen pattern from papillary to reticular. Further, with the increase in Gleason score, collagen fibers presented higher orientated and stiffened (Ling et al. 2017; Yuting et al. 2018). Other study demonstrated that shorter collagen fibers and loss of fiber alignment was correlated with unfavorable prognosis (Sridharan et al. 2015).

Lung pathology
Collagen fiber distribution and SHG intensity of fibers vary in different areas of the normal lung. Thus, large areas of the organ should be scanned to allow distinction between tumor and non-tumor regions using SHG microscopy.

Lung squamous cell carcinoma showed fewer elastin and collagen fibers compared to normal tissue. In desmoplastic areas, however, significantly larger total amounts and longer fibers of collagen were detected (Xu et al. 2013). Besides, amount of collagen fibers and the spread of fibers towards the dominant direction represented an indicator of disorder in tumor matrix (Golaraei et al. 2014), promoting higher stiffness and EMT (Pankova et al. 2019).

Brain
Glioblastoma xenograft model has shown that in normal brain parenchyma only low amounts of collagen exist, mainly around part of the blood vessels. Differences in focal and invasive tumors were observed: (1) in focal tumors, collagen appeared to encapsulate neoplasia at the transition with normal tissue, and (2) in invasive tumors, collagen appeared intertwined within the tumor cell groups. Focal tumors showed more organized collagen, based on the presence of more aligned, longer, wider and straighter collagen fibers, than animals with invasive tumors (Pointer et al. 2017). In humans, tumors with less organized collagen were associated with unfavorable outcomes (Pointer et al. 2017).

Thyroid pathology
In normal thyroid tissue collagen was deposited in a fine and linear pattern, while in neoplasia fibers were wavy and thick (Huang et al. 2010). In addition, thyroid carcinoma presented greater disorganization of the fibers, both at structural and ultrastructural levels (Tokarz et al. 2015). Further, collagen deposition pattern in the thyroid capsule could distinguish between benign and malignant nodules, i.e., follicular adenoma and papillary thyroid carcinoma (Hristu et al. 2018). Collagen fiber organization was similar between two histological variants of papillary thyroid carcinoma, the classical and the follicular, both with similar prognoses (Passler et al. 2003; Yu et al. 2013).

Dermatology pathology
In melanoma, collagen evaluation might represent a rapid and reliable method for defining the borders of the lesions and the extent of dermal invasion (Breslow thickness), as collagen density in the transition from melanoma to unaltered tissue was shown to gradually increase. Additionally, the evaluation of collagen fiber structure presented high degree of concordance with the evaluation of H&E and Melan-A stained tissue specimens by the pathologists (Thrasivoulou et al. 2011). Clusters of malignant melanocytes were associated with absence of collagen, probably due to its destruction by metalloproteinases. In areas related to melanoma, collagen morphology was greatly affected, namely, with very short and

thin fibers. SHG signals gradually intensified from the transition of neoplasia to normal tissues (Thrasivoulou et al. 2011) (Fig. 5). In a melanoma xenograft model, it was also demonstrated that the amount and orientation of collagen fibers diminished as melanoma progressed (Wu et al. 2015). Similar collagen patterns were described in squamous and basal cell carcinomas (Heuke et al. 2013; Lin et al. 2006).

Discussion and conclusion

The present manuscript comprises some of the applications of SHG microscopy in Oncologic Pathology, mainly in the study of ECM of epithelial tumors. Herein, it was shown how collagen parameters measured by this technique could aid in the differential diagnosis and in prognostic stratification of different cancer types. There is evidence for the association between higher amount, lower organization and higher linearity of collagen fibers, and tumor progression and metastasizing.

Although increased deposition of collagen fibers may be a predictor of progression (Drifka et al. 2015; Kakkad et al. 2012; Pal et al. 2015; Vargas et al. 2009), it should be noted that post therapeutic tissue changes and desmoplastic reaction may mimic such an increase in collagen fibers (Li et al. 2017). Therefore, other parameters of collagen, as alignment and organization, are essential for a more specific evaluation of collagen structure deposited. Such collagen parameters are better evaluated by SHG microscopy. The explanation on the mechanisms by which structure is associated with biological behavior

Fig. 5 Melanoma specimen. Yellow dashed line represents cluster of neoplastic cells. Transition with neoplastic cell aggregates shows reduced amount of collagen. Stroma more distant to tumor presents increasing amounts of collagen

could be explored in functional studies, briefly discussed in the following paragraphs.

It was demonstrated that high collagen fiber linearity (stretched collagen fibers) enhanced motility of neoplastic cells, by increasing directional persistence and restricting protrusions along aligned fibers, thus promoting greater distance traveled by cancer cell (Riching et al. 2014). Experimental modulation of collagen fibers organization through an anti-lysyl oxidase-like-2 antibody evidenced that ECM composition remained unaltered, while the resulting alteration in collagen fibers structure interfered with neoplastic cell adhesion and invasion properties, reducing primary tumor growth (Grossman et al. 2016). Also, it was indicated that expression of collagen prolyl-hydroxylases promoted cancer cell alignment along collagen fibers, resulting in enhanced invasion and metastasis to lymph nodes and lungs. Finally, it was established that the expression of collagen prolyl-hydroxylase mRNA in biopsies of human breast cancer was associated with prognosis, and that ethyl-3,4-dihydroxybenzoate, a prolyl-hydroxylase inhibitor, was associated with decreased tumor fibrosis and metastasizing in a mouse model of breast cancer (Gilkes et al. 2013). Moreover, cancer-associated adipocytes (CAAs) were shown to remodel collagen alignment in crosstalk with breast cancer cell, further promoting breast cancer metastasis. Tumor derived plasminogen activator inhibitor-1 (PAI-1) was required to activate the expression of the intracellular enzyme procollagen-lysine, 2-oxoglutarate 5-dioxygenase 2 (PLOD2) in CAAs (Wei et al. 2019). Further, tumor-associated macrophages (TAMs) regulate tumor sustained growth by secreting type I collagen, which can activate prosurvival signals produced by the integrin $\alpha2\beta1$/PI3K/AKT signaling pathway (Qiu et al. 2019).

Overall literature data on breast cancer point to the association between higher deposition of collagen and worse prognosis, regardless of the model used (i.e., mice (Provenzano et al. 2008), dog (Case et al. 2017) and human (Natal et al. 2018b)). One possible explanation is that increase in collagen density might reduce activation of STAT5 in neoplastic cells, leading to an increase in phosphorylated ERK 1/2 and Akt proteins that, consequently, would promote tumor growth (Barcus et al. 2017). In this line, the association between increased breast cancer risk and obesity could be at least partially explained by the increased collagen deposition and stiffness in the breast of obese patients (Le et al. 2007). In contrast, reduction of linearity and rigidity of collagen promoted in the nursing breast, could be related to its reduced risk for cancer (Maller et al. 2013). Further, COL1A1 was up-regulated in microinvasive breast carcinoma and its knockdown significantly inhibited the proliferation, migration, and invasion by inhibiting EMT
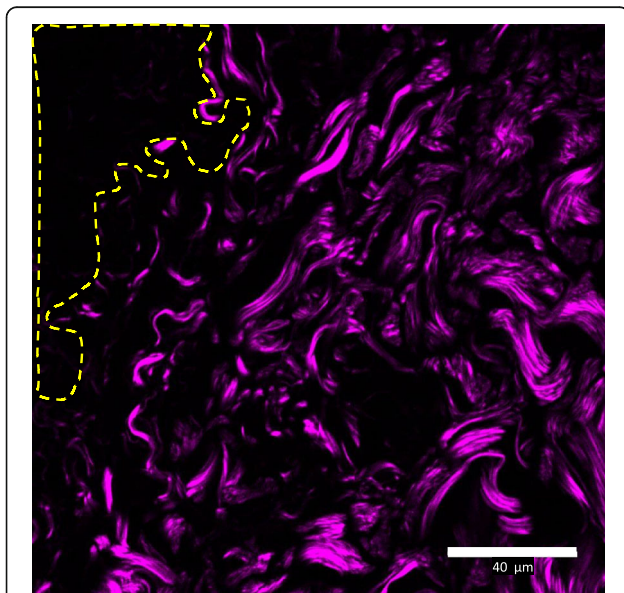
process and the TGF-β signaling pathway (Zhu et al. 2019).

Additionally, it was observed that collagen fibers alignment conferred increased stiffness, thus promoting EMT by an essential mechanomediator, TWIST1, a basic helix-loop-helix transcription factor (Riching et al. 2014; Wei et al. 2015). In this case, high matrix stiffness promoted nuclear translocation of TWIST1 by releasing it from its cytoplasmic binding partner G3BP2. Loss of G3BP2 leads to constitutive TWIST1 nuclear localization and synergizes with increasing matrix stiffness to induce EMT and promote tumor invasion and metastasis. In human breast tumors, collagen fiber alignment, a marker of increasing matrix stiffness, together with reduced expression of G3BP2 predicted poor survival. It was revealed that a TWIST1–G3BP2 mechanotransduction pathway, responsive biomechanical signals from the TME, could drive EMT, invasion, and metastasis [105]. Further, it was shown that the oriented fibers greatly enhance and facilitate the metastatic cell intravasation process during metastasis (Han et al. 2016).

In a human non-small cell lung carcinoma cell line model in collagen gel, inhibition of LKB1 or MARK1 increased collagen fiber alignment, that is, increased tumor invasiveness (Lee et al. 2017). Mutations of LKB1 are detected in various tumors. This protein interacts with MARK1 to regulate collagen remodeling and cancer cell motility, thus explaining their influence on tumor behavior. This is probably related to another mechanism of cell migration, which is independent of soluble factors, the Rho-associated kinase (ROCK)-mediated contractility, required for collagen alignment and cell migration (Drifka et al. 2016a, b). In other experiment using human lung adenocarcinoma it was described that promoter methylation of RASSF1A, a key regulator of the Hippo pathway, promoted nuclear accumulation of YAP1, and expression of prolyl 4-hydroxylase alpha-2 (P4HA2) (Pankova et al. 2019). P4HA2 is known to have a major effect on physical properties of tumor-associated ECM, which in turn leads to increased organization and stiffness of collagen structure during cancer progression (Levental et al. 2009b; Provenzano et al. 2006b). Further, it was identified that elevated collagen creates a stiff ECM which in turn triggers cancer stem-like programming and metastatic dissemination. Although, re-expression of RASSF1A or inhibition of P4HA2 activity reverses these effects and increases markers of lung differentiation (TTF-1 and Mucin 5B) (Pankova et al. 2019).

The hepatitis B virus X protein (HBx) is essential for HBV replication and is thought to play a major role in HCC (Kremsdorf et al. 2006). HBx expression potentiates liver fibrosis with increased expression of proteins involved in matrix remodeling, such as collagen, and

inflammatory cytokines, such as TNF-α. This correlated with a higher expression of tumor progenitor cell markers (AFP, Ly6D and EpCam), indicating a higher risk of progression from fibrosis to HCC (Ahodantin et al. 2019).

However, it was shown that ionizing radiation could reduce the stiffness collagen matrix. When non-irradiated cancer cells were seeded in an irradiated matrix, adhesion, spreading, and migration were reduced (Miller et al. 2018). In contrast, there are cases where the greater amount of collagen fibers deposited or their greater alignment is related to a better prognosis, and their loss may be associated with tumor progression. This is especially true for glioblastoma (Pointer et al. 2017), a tumor with important differences in comparison with epithelial tumors.

In conclusion, cancer progression and metastasizing represent complex processes, in which matrix remodeling plays a central role, together with cancer cell genetic modifications. Integration of studies on cancer cell biology and ECM are highly advantageous to give us a more complete picture of these processes. As microscopic techniques provide topographic information allied with biologic characteristics of tissue components, they represent important tools for a more complete understanding of cancer progression. In this context, SHG has provided significant insights in human tumor specimens, readily available for Pathologists.

Abbreviations
CAA: Cancer-associated adipocytes; ECM: Extracellular matrix; EMT: Epithelial-to-mesenchymal transition; HCC: Hepatocellular carcinoma; HER-2: Human epidermal growth factor receptor 2; P4HA2: Prolyl 4-hydroxylase alpha-2; PAI-1: Plasminogen activator inhibitor-1; PLOD-1: Procollagen-lysine, 2-oxoglutarate 5-dioxygenase 2; ROCK: Rho-associated kinase; SHG: Second-harmonic generation; TACS: Tumor associated collagen signature; TAM: Tumor-associated macrophages; THG: Third-harmonic generation; TMA: Tissue microarray; TME: Tumor microenvironment; TPEF: Tow-photons excited fluorescence

Declarations

Competing interests
The authors declare that they have no competing interests.

Author details
[1]Laboratory of Investigative and Molecular Pathology, Faculty of Medical Sciences, University of Campinas. Rua Tessália Vieira de Camargo, 126, Zip code: 13083-970, Campinas, São Paulo, Brazil. [2]Instituto de Investigación y Deasrrollo en Bioingeniería y Bioinformática (IBB), Universidad Nacional de Entre Ríos, Concepción del Uruguay, Entre Ríos, Argentina. [3]Department of Quantum Electronics, Institute of Physics "Gleb Wataghin", University of Campinas, Campinas, São Paulo, Brazil. [4]Department of Physics, Federal University of Ceará, Fortaleza, Ceará, Brazil. [5]Consultant Pathologist at the Laboratory of Pathology, Rede D'Or Hospital, São Paulo, Brazil.

References
Adur J (2012) Quantitative changes in human epithelial cancers and osteogenesis imperfecta disease detected using nonlinear multicontrast microscopy. J Biomed Opt 17:081407. https://doi.org/10.1117/1.jbo.17.8.081407

Adur J, Pelegati VB, de Thomaz AA, Baratti MO, Almeida DB, Andrade LALA, Bottcher-Luiz F, Carvalho HF, Cesar CL (2012) Optical biomarkers of serous and mucinous human ovarian tumor assessed with nonlinear optics microscopies. PLoS One 7:e47007. https://doi.org/10.1371/journal.pone.0047007

Adur J, Pelegati VB, de Thomaz AA, Baratti MO, Andrade LALA, Carvalho HF, Bottcher-Luiz F, Cesar CL (2014) Second harmonic generation microscopy as a powerful diagnostic imaging modality for human ovarian cancer. J Biophotonics 7:37–48. https://doi.org/10.1002/jbio.201200108

Ahodantin J, Lekbaby B, Bou Nader M, Soussan P, Kremsdorf D (2019) Hepatitis B virus X protein enhances the development of liver fibrosis and the expression of genes associated with epithelial-mesenchymal transitions and tumor progenitor cells. Carcinogenesis. https://doi.org/10.1093/carcin/bgz109

Barcus CE, O'Leary KA, Brockman JL, Rugowski DE, Liu Y, Garcia N, Yu M, Keely PJ, Eliceiri KW, Schuler LA (2017) Elevated collagen-I augments tumor progressive signals, intravasation and metastasis of prolactin-induced estrogen receptor alpha positive mammary tumor cells. Breast Cancer Res 19:9. https://doi.org/10.1186/s13058-017-0801-1

Best SL, Liu Y, Keikhosravi A, Drifka CR, Woo KM, Mehta GS, Altwegg M, Thimm TN, Houlihan M, Bredfeldt JS, Abel EJ, Huang W, Eliceiri KW (2019) Collagen organization of renal cell carcinoma differs between low and high grade tumors. BMC Cancer 19:490. https://doi.org/10.1186/s12885-019-5708-z

Boyd NF, Dite GS, Stone J, Gunasekara A, English DR, McCredie MRE, Giles GG, Tritchler D, Chiarelli A, Yaffe MJ, Hopper JL (2002) Heritability of mammographic density, a risk factor for breast cancer. N Engl J Med 347: 886–894. https://doi.org/10.1056/NEJMoa013390

Brabrand A, Kariuki II, Engstrøm MJ, Haugen OA, Dyrnes LA, Åsvold BO, Lilledahl MB, Bofin AM (2015) Alterations in collagen fibre patterns in breast cancer. A premise for tumour invasiveness? APMIS 123:1–8. https://doi.org/10.1111/apm.12298

Bredfeldt JS, Liu Y, Conklin MW, Keely PJ, Mackie TR, Eliceiri KW (2014) Automated quantification of aligned collagen for human breast carcinoma prognosis. J Pathol Inform 5:28. https://doi.org/10.4103/2153-3539.139707

Brooks M, Mo Q, Krasnow R, Ho PL, Lee Y-C, Xiao J, Kurtova A, Lerner S, Godoy G, Jian W, Castro P, Chen F, Rowley D, Ittmann M, Chan KS (2016) Positive association of collagen type I with non-muscle invasive bladder cancer progression. Oncotarget 7:82609–82619. https://doi.org/10.18632/oncotarget.12089

Campagnola PJ, Clark HA, Mohler WA, Lewis A, Loew LM (2001) Second-harmonic imaging microscopy of living cells. J Biomed Opt 6:277. https://doi.org/10.1117/1.1383294

Campagnola PJ, Millard AC, Terasaki M, Hoppe PE, Malone CJ, Mohler WA (2002) Three-dimensional high-resolution second-harmonic generation imaging of endogenous structural proteins in biological tissues. Biophys J 82:493–508. https://doi.org/10.1016/S0006-3495(02)75414-3

Campbell KR, Campagnola PJ (2017) Assessing local stromal alterations in human ovarian cancer subtypes via second harmonic generation microscopy and analysis. J Biomed Opt 22:1–7. https://doi.org/10.1117/1.JBO.22.11.116008

Case A, Brisson BK, Durham AC, Rosen S, Monslow J, Buza E, Salah P, Gillem J, Ruthel G, Veluvolu S, Kristiansen V, Puré E, Brown DC, Sørenmo KU, Volk SW (2017) Identification of prognostic collagen signatures and potential therapeutic stromal targets in canine mammary gland carcinoma. PLoS One 12:e0180448. https://doi.org/10.1371/journal.pone.0180448

Chang HY, Nuyten DSA, Sneddon JB, Hastie T, Tibshirani R, Sørlie T, Dai H, He YD, van't Veer LJ, Bartelink H, van de Rijn M, Brown PO, van de Vijver MJ (2005) Robustness, scalability, and integration of a wound-response gene expression signature in predicting breast cancer survival. Proc Natl Acad Sci U S A 102: 3738–3743. https://doi.org/10.1073/pnas.0409462102

Chang HY, Sneddon JB, Alizadeh AA, Sood R, West RB, Montgomery K, Chi J-T, van de Rijn M, Botstein D, Brown PO (2004) Gene expression signature of fibroblast serum response predicts human cancer progression: similarities between tumors and wounds. PLoS Biol 2:E7. https://doi.org/10.1371/journal.pbio.0020007

Chen D, Chen G, Jiang W, Fu M, Liu W, Sui J, Xu S, Liu Z, Zheng X, Chi L, Lin D, Li K, Chen W, Zuo N, Lu J, Chen J, Li G, Zhuo S, Yan J (2019) Association of the collagen signature in the tumor microenvironment with lymph node metastasis in early gastric cancer. JAMA Surg 154:1–9. https://doi.org/10.1001/jamasurg.2018.5249

Chen WS, Wang Y, Liu NR, Zhang JX, Chen R (2014) Multiphoton microscopic imaging of human normal and cancerous oesophagus tissue. J Microsc 253: 79–82. https://doi.org/10.1111/jmi.12102

Colpaert CG, Vermeulen PB, Fox SB, Harris AL, Dirix LY, Van Marck EA (2003) The presence of a fibrotic focus in invasive breast carcinoma correlates with the expression of carbonic anhydrase IX and is a marker of hypoxia and poor prognosis. Breast Cancer Res Treat 81:137–147. https://doi.org/10.1023/A:1025702330207

Conklin MW, Eickhoff JC, Riching KM, Pehlke CA, Eliceiri KW, Provenzano PP, Friedl A, Keely PJ (2011) Aligned collagen is a prognostic signature for survival in human breast carcinoma. Am J Pathol 178:1221–1232. https://doi.org/10.1016/j.ajpath.2010.11.076

Conklin MW, Gangnon RE, Sprague BL, Van Gemert L, Hampton JM, Eliceiri KW, Bredfeldt JS, Liu Y, Surachaicharn N, Newcomb PA, Friedl A, Keely PJ, Trentham-Dietz A (2018) Collagen alignment as a predictor of recurrence after ductal carcinoma in situ. Cancer Epidemiol Biomarkers Prev 27:138–145. https://doi.org/10.1158/1055-9965.EPI-17-0720

Cox G (2011) Biological applications of second harmonic imaging. Biophys Rev 3: 131. https://doi.org/10.1007/s12551-011-0052-9

Dombeck DA, Kasischke KA, Vishwasrao HD, Ingelsson M, Hyman BT, Webb WW (2003) Uniform polarity microtubule assemblies imaged in native brain tissue by second-harmonic generation microscopy. Proc Natl Acad Sci 100:7081–7086. https://doi.org/10.1073/pnas.0731953100

Drifka CR, Tod J, Loeffler AG, Liu Y, Thomas GJ, Eliceiri KW, Kao WJ (2015) Periductal stromal collagen topology of pancreatic ductal adenocarcinoma differs from that of normal and chronic pancreatitis. Mod Pathol 28:1470–1480. https://doi.org/10.1038/modpathol.2015.97

Drifka CR, Loeffler AG, Esquibel CR, Weber SM, Eliceiri KW, Kao WJ (2016a) Human pancreatic stellate cells modulate 3D collagen alignment to promote the migration of pancreatic ductal adenocarcinoma cells. Biomed Microdevices 18:105. https://doi.org/10.1007/s10544-016-0128-1

Drifka CR, Loeffler AG, Mathewson K, Keikhosravi A, Eickhoff JC, Liu Y, Weber SM, Kao WJ, Eliceiri KW (2016b) Highly aligned stromal collagen is a negative prognostic factor following pancreatic ductal adenocarcinoma resection. Oncotarget 7:76197–76213. https://doi.org/10.18632/oncotarget.12772

Finak G, Bertos N, Pepin F, Sadekova S, Souleimanova M, Zhao H, Chen H, Omeroglu G, Meterissian S, Omeroglu A, Hallett M, Park M (2008) Stromal gene expression predicts clinical outcome in breast cancer. Nat Med 14:518–527. https://doi.org/10.1038/nm1764

Fraley SI, Feng Y, Giri A, Longmore GD, Wirtz D (2012) Dimensional and temporal controls of three-dimensional cell migration by zyxin and binding partners. Nat Commun 3:719. https://doi.org/10.1038/ncomms1711

Fraley SI, Feng Y, Krishnamurthy R, Kim D-H, Celedon A, Longmore GD, Wirtz D (2010) A distinctive role for focal adhesion proteins in three-dimensional cell motility. Nat Cell Biol 12:598–604. https://doi.org/10.1038/ncb2062

Frantz C, Stewart KM, Weaver VM (2010) The extracellular matrix at a glance. J Cell Sci 123:4195–4200. https://doi.org/10.1242/jcs.023820

Freund I, Deutsch M (1986) Second-harmonic microscopy of biological tissue. Opt Lett 11:94

Gilkes DM, Chaturvedi P, Bajpai S, Wong CC, Wei H, Pitcairn S, Hubbi ME, Wirtz D, Semenza GL (2013) Collagen Prolyl hydroxylases are essential for breast cancer metastasis. Cancer Res 73:3285–3296. https://doi.org/10.1158/0008-5472.CAN-12-3963

Golaraei A, Cisek R, Krouglov S, Navab R, Niu C, Sakashita S, Yasufuku K, Tsao M-S, Wilson BC, Barzda V (2014) Characterization of collagen in non-small cell lung

carcinoma with second harmonic polarization microscopy. Biomed Opt Express 5:3562–3567. https://doi.org/10.1364/BOE.5.003562

Golaraei A, Kontenis L, Cisek R, Tokarz D, Done SJ, Wilson BC, Barzda V (2016) Changes of collagen ultrastructure in breast cancer tissue determined by second-harmonic generation double stokes-Mueller polarimetric microscopy. Biomed Opt Express 7:4054–4068. https://doi.org/10.1364/BOE.7.004054

Gould VE, Koukoulis GK, Virtanen I (1990) Extracellular matrix proteins and their receptors in the normal, hyperplastic and neoplastic breast. Cell Differ Dev 32:409–416

Grossman M, Ben-Chetrit N, Zhuravlev A, Afik R, Bassat E, Solomonov I, Yarden Y, Sagi I (2016) Tumor cell invasion can be blocked by modulators of collagen fibril alignment that control assembly of the extracellular matrix. Cancer Res 76:4249–4258. https://doi.org/10.1158/0008-5472.CAN-15-2813

Han W, Chen S, Yuan W, Fan Q, Tian J, Wang X, Chen L, Zhang X, Wei W, Liu R, Qu J, Jiao Y, Austin RH, Liu L (2016) Oriented collagen fibers direct tumor cell intravasation. Proc Natl Acad Sci U S A 113:11208–11213. https://doi.org/10.1073/pnas.1610347113

Hasebe T, Tsuda H, Tsubono Y, Imoto S, Mukai K (1997) Fibrotic focus in invasive ductal carcinoma of the breast: a histopathological prognostic parameter for tumor recurrence and tumor death within three years after the initial operation. Jpn J Cancer Res 88:590–599

Heuke S, Vogler N, Meyer T, Akimov D, Kluschke F, Röwert-Huber H-J, Lademann J, Dietzek B, Popp J (2013) Detection and discrimination of non-melanoma skin cancer by multimodal imaging. Healthc (Basel, Switzerland) 1:64–83. https://doi.org/10.3390/healthcare1010064

Hollern DP, Andrechek ER (2014) A genomic analysis of mouse models of breast cancer reveals molecular features of mouse models and relationships to human breast cancer. Breast Cancer Res 16:R59. https://doi.org/10.1186/bcr3672

Hristu R, Eftimie LG, Stanciu SG, Tranca DE, Paun B, Sajin M, Stanciu GA (2018) Quantitative second harmonic generation microscopy for the structural characterization of capsular collagen in thyroid neoplasms. Biomed Opt Express 9:3923–3936. https://doi.org/10.1364/BOE.9.003923

Huang Z, Li Z, Chen R, Lin J, Li Y, Li C (2010) *In Vitro* imaging of thyroid tissues using two-photon excited fluorescence and second harmonic generation. Photomed Laser Surg 28:S-129–S-133. https://doi.org/10.1089/pho.2009.2563

Huijbers IJ, Iravani M, Popov S, Robertson D, Al-Sarraj S, Jones C, Isacke CM (2010) A role for fibrillar collagen deposition and the collagen internalization receptor endo180 in glioma invasion. PLoS One 5:e9808. https://doi.org/10.1371/journal.pone.0009808

Kakkad SM, Solaiyappan M, Argani P, Sukumar S, Jacobs LK, Leibfritz D, Bhujwalla ZM, Glunde K (2012) Collagen I fiber density increases in lymph node positive breast cancers: pilot study. J Biomed Opt 17:116017. https://doi.org/10.1117/1.JBO.17.11.116017

Kalies S, Kuetemeyer K, Heisterkamp A (2011) Mechanisms of high-order photobleaching and its relationship to intracellular ablation. Biomed Opt Express 2:805–816. https://doi.org/10.1364/BOE.2.000816

Kauppila S, Stenbäck F, Risteli J, Jukkola A, Risteli L (1998) Aberrant type I and type III collagen gene expression in human breast cancer in vivo. J Pathol 186:262–268. https://doi.org/10.1002/(SICI)1096-9896(1998110)186:3<262::AID-PATH191>3.0.CO;2-3

Kirkpatrick ND, Brewer MA, Utzinger U (2007) Endogenous optical biomarkers of ovarian cancer evaluated with multiphoton microscopy. Cancer Epidemiol Biomarkers Prev 16:2048–2057. https://doi.org/10.1158/1055-9965.EPI-07-0009

Kremsdorf D, Soussan P, Paterlini-Brechot P, Brechot C (2006) Hepatitis B virus-related hepatocellular carcinoma: paradigms for viral-related human carcinogenesis. Oncogene 25:3823–3833. https://doi.org/10.1038/sj.onc.1209559

Le TT, Rehrer CW, Huff TB, Nichols MB, Camarillo IG, Cheng J-X (2007) Nonlinear optical imaging to evaluate the impact of obesity on mammary gland and tumor stroma. Mol Imaging 6:205–211

Lee B, Konen J, Wilkinson S, Marcus AI, Jiang Y (2017) Local alignment vectors reveal cancer cell-induced ECM fiber remodeling dynamics. Sci Rep 7:39498. https://doi.org/10.1038/srep39498

Levental KR, Yu H, Kass L, Lakins JN, Egeblad M, Erler JT, Fong SFT, Csiszar K, Giaccia A, Weninger W, Yamauchi M, Gasser DL, Weaver VM (2009a) Matrix crosslinking forces tumor progression by enhancing integrin signaling. Cell 139:891–906. https://doi.org/10.1016/j.cell.2009.10.027

Li L-H, Chen Z-F, Wang X-F, Liu X, Jiang W-Z, Zhuo S-M, Jiang L-W, Guan G-X, Chen J-X, Li L-H, Chen Z-F, Wang X-F, Liu X, Jiang W-Z, Zhuo S-M, Jiang L-W, Guan G-X, Chen J-X (2017) Monitoring neoadjuvant therapy responses in rectal cancer using multimodal nonlinear optical microscopy. Oncotarget 8: 107323–107333. https://doi.org/10.18632/oncotarget.22366

Lin H, Lin L, Wang G, Zuo N, Zhan Z, Xie S, Chen G, Chen J, Zhuo S (2018) Label-free classification of hepatocellular-carcinoma grading using second harmonic generation microscopy. Biomed Opt Express 9:3783–3793. https://doi.org/10.1364/BOE.9.003783

Lin S-J, Jee S-H, Kuo C-J, Wu R-J, Lin W-C, Chen J-S, Liao Y-H, Hsu C-J, Tsai T-F, Chen Y-F, Dong C-Y (2006) Discrimination of basal cell carcinoma from normal dermal stroma by quantitative multiphoton imaging. Opt Lett 31: 2756. https://doi.org/10.1364/OL.31.002756

Ling Y, Li C, Feng K, Palmer S, Appleton PL, Lang S, McGloin D, Huang Z, Nabi G (2017) Second harmonic generation (SHG) imaging of cancer heterogeneity in ultrasound guided biopsies of prostate in men suspected with prostate cancer. J Biophotonics 10:911–918. https://doi.org/10.1002/jbio.201600090

Liu N, Chen J, Xu R, Jiang S, Xu J, Chen R (2013) Label-free imaging characteristics of colonic mucinous adenocarcinoma using multiphoton microscopy. Scanning 35:277–282. https://doi.org/10.1002/sca.21063

Ma H-P, Chang H-L, Bamodu OA, Yadav VK, Huang T-Y, Wu ATH, Yeh C-T, Tsai S-H, Lee W-H (2019) Collagen 1A1 (COL1A1) is a reliable biomarker and putative therapeutic target for hepatocellular carcinogenesis and metastasis. Cancers (Basel) 11:786. https://doi.org/10.3390/cancers11060786

Maier F, Siri S, Santos S, Chen L, Feng B, Pierce DM (2021) The heterogeneous morphology of networked collagen in distal colon and rectum of mice quantified via nonlinear microscopy. J Mech Behav Biomed Mater 113: 104116. https://doi.org/10.1016/j.jmbbm.2020.104116

Maller O, Hansen KC, Lyons TR, Acerbi I, Weaver VM, Prekeris R, Tan A-C, Schedin P (2013) Collagen architecture in pregnancy-induced protection from breast cancer. J Cell Sci 126:4108–4110. https://doi.org/10.1242/jcs.121590

Mehravar S, Banerjee B, Chatrath H, Amirsolaimani B, Patel K, Patel C, Norwood RA, Peyghambarian N, Kieu K (2016) Label-free multi-photon imaging of dysplasia in Barrett's esophagus. Biomed Opt Express 7:148–157. https://doi.org/10.1364/BOE.7.000148

Miller JP, Borde BH, Bordeleau F, Zanotelli MR, LaValley DJ, Parker DJ, Bonassar LJ, Pannullo SC, Reinhart-King CA (2018) Clinical doses of radiation reduce collagen matrix stiffness. APL Bioeng 2:031901. https://doi.org/10.1063/1.5018327

Müller, Squier, Wilson, Brakenhoff (1998) 3D microscopy of transparent objects using third-harmonic generation. J Microsc 191:266–274

Naba A, Clauser KR, Hoersch S, Liu H, Carr SA, Hynes RO (2012) The matrisome: in silico definition and in vivo characterization by proteomics of normal and tumor extracellular matrices. Mol Cell Proteomics 11:M111.014647. https://doi.org/10.1074/mcp.M111.014647

Nadiarnykh O, LaComb RB, Brewer MA, Campagnola PJ (2010) Alterations of the extracellular matrix in ovarian cancer studied by second harmonic generation imaging microscopy. BMC Cancer 10:94. https://doi.org/10.1186/1471-2407-10-94

Natal R d A, Paiva GR, Pelegati VB, Marenco L, Alvarenga CA, Vargas RF, Derchain SF, Sarian LO, Franchet C, Cesar CL, Schmitt FC, Weigelt B, Vassallo J (2019) Exploring collagen parameters in pure special types of invasive breast cancer. Sci Rep 9. https://doi.org/10.1038/s41598-019-44156-9

Natal RA, Vassallo J, Paiva GR, Pelegati VB, Barbosa GO, Mendonça GR, Bondarik C, Derchain SF, Carvalho HF, Lima CS, Cesar CL, Sarian LO (2018a) Collagen analysis by second-harmonic generation microscopy predicts outcome of luminal breast cancer. Tumor Biol 40:101042831877095. https://doi.org/10.1177/1010428318770953

Natal RA, Vassallo J, Paiva GR, Pelegati VB, Barbosa GO, Mendonça GR, Bondarik C, Derchain SF, Carvalho HF, Lima CS, Cesar CL, Sarian LO (2018b) Collagen analysis by second-harmonic generation microscopy predicts outcome of luminal breast cancer. Tumour Biol 40:1010428318770953. https://doi.org/10.1177/1010428318770953

Nie YT, Wu Y, Fu FM, Lian YE, Zhuo SM, Wang C, Chen JX (2015) Differentiating the two main histologic categories of fibroadenoma tissue from normal breast tissue by using multiphoton microscopy. J Microsc 258:79–85. https://doi.org/10.1111/jmi.12219

Pal R, Yang J, Ortiz D, Qiu S, Resto V, McCammon S, Vargas G (2015) In-vivo nonlinear optical microscopy (NLOM) of epithelial-connective tissue interface (ECTI) reveals quantitative measures of neoplasia in hamster oral mucosa. PLoS One 10:e0116754. https://doi.org/10.1371/journal.pone.0116754

Pankova D, Jiang Y, Chatzifrangkeskou M, Vendrell I, Buzzelli J, Ryan A, Brown C, O'Neill E (2019) RASSF1A controls tissue stiffness and cancer stem-like cells in lung adenocarcinoma. EMBO J 38:e100532. https://doi.org/10.15252/embj.2018100532

Passler C, Prager G, Scheuba C, Niederle BE, Kaserer K, Zettinig G, Niederle B (2003) Follicular variant of papillary thyroid carcinoma. Arch Surg 138:1362. https://doi.org/10.1001/archsurg.138.12.1362

Paszek MJ, Zahir N, Johnson KR, Lakins JN, Rozenberg GI, Gefen A, Reinhart-King CA, Margulies SS, Dembo M, Boettiger D, Hammer DA, Weaver VM (2005) Tensional homeostasis and the malignant phenotype. Cancer Cell 8:241–254. https://doi.org/10.1016/j.ccr.2005.08.010

Patterson GH, Piston DW (2000) Photobleaching in two-photon excitation microscopy. Biophys J 78:2159–2162. https://doi.org/10.1016/S0006-3495(00)76762-2

Pointer KB, Clark PA, Schroeder AB, Salamat MS, Eliceiri KW, Kuo JS (2017) Association of collagen architecture with glioblastoma patient survival. J Neurosurg 126:1812–1821. https://doi.org/10.3171/2016.6.JNS152797

Provenzano PP, Eliceiri KW, Campbell JM, Inman DR, White JG, Keely PJ (2006a) Collagen reorganization at the tumor-stromal interface facilitates local invasion. BMC Med 4:38. https://doi.org/10.1186/1741-7015-4-38

Provenzano PP, Inman DR, Eliceiri KW, Knittel JG, Yan L, Rueden CT, White JG, Keely PJ (2008) Collagen density promotes mammary tumor initiation and progression. BMC Med 6:11. https://doi.org/10.1186/1741-7015-6-11

Qiu J, Jiang W, Yang Y, Feng C, Chen Z, Guan G, Zhuo S, Chen J (2015) Monitoring changes of tumor microenvironment in colorectal submucosa using multiphoton microscopy. Scanning 37:17–22. https://doi.org/10.1002/sca.21174

Qiu S, Deng L, Liao X, Nie L, Qi F, Jin K, Tu X, Zheng X, Li J, Liu L, Liu Z, Bao Y, Ai J, Lin T, Yang L, Wei Q (2019) Tumor associated macrophages promote bladder tumor growth through PI 3k/ AKT signal induced by collagen. Cancer Sci 110:cas.14078. https://doi.org/10.1111/cas.14078

Ramaswamy S, Ross KN, Lander ES, Golub TR (2003) A molecular signature of metastasis in primary solid tumors. Nat Genet 33:49–54. https://doi.org/10.1038/ng1060

Riching KM, Cox BL, Salick MR, Pehlke C, Riching AS, Ponik SM, Bass BR, Crone WC, Jiang Y, Weaver AM, Eliceiri KW, Keely PJ (2014) 3D collagen alignment limits protrusions to enhance breast cancer cell persistence. Biophys J 107:2546–2558. https://doi.org/10.1016/J.BPJ.2014.10.035

Sheppard CJR, Kompfner R (1978) Resonant scanning optical microscope. Appl Optics 17:2879. https://doi.org/10.1364/AO.17.002879

Sridharan S, Macias V, Tangella K, Kajdacsy-Balla A, Popescu G (2015) Prediction of prostate cancer recurrence using quantitative phase imaging. Sci Rep 5:9976. https://doi.org/10.1038/srep09976

Tajik S (2018) Application of Cu (II) nanocomplex modified graphite screen printed electrode to improve the sensitivity for norepinephrine detection. Anal Bioanal Electrochem 10:778–788. https://doi.org/10.1126/science.2321027

Tan WJ, Yan J, Xu S, Thike AA, Bay BH, Yu H, Tan M-H, Tan PH (2015) Second harmonic generation microscopy is a novel technique for differential diagnosis of breast fibroepithelial lesions. J Clin Pathol 68:1033–1035. https://doi.org/10.1136/jclinpath-2015-203231

Thrasivoulou C, Virich G, Krenacs T, Korom I, Becker DL (2011) Optical delineation of human malignant melanoma using second harmonic imaging of collagen. Biomed Opt Express 2:1282–1295. https://doi.org/10.1364/BOE.2.001282

Tilbury KB, Campbell KR, Eliceiri KW, Salih SM, Patankar M, Campagnola PJ (2017) Stromal alterations in ovarian cancers via wavelength dependent second harmonic generation microscopy and optical scattering. BMC Cancer 17:102. https://doi.org/10.1186/s12885-017-3090-2

Tokarz D, Cisek R, Golaraei A, Asa SL, Barzda V, Wilson BC (2015) Ultrastructural features of collagen in thyroid carcinoma tissue observed by polarization second harmonic generation microscopy. Biomed Opt Express 6:3475–3481. https://doi.org/10.1364/BOE.6.003475

Ustione A, Piston DW (2011) A simple introduction to multiphoton microscopy. J Microsc 243:221–226. https://doi.org/10.1111/j.1365-2818.2011.03532.x

van der Rest M, Garrone R (1991) Collagen family of proteins. FASEB J 5:2814–2823

van Kempen LCLT, Ruiter DJ, van Muijen GNP, Coussens LM (2003) The tumor microenvironment: a critical determinant of neoplastic evolution. Eur J Cell Biol 82:539–548. https://doi.org/10.1078/0171-9335-00346

Vargas G, Shilagard T, Ki-Hong Ho K-H, McCammon S (2009). Multiphoton autofluorescence microscopy and second harmonic generation microscopy of oral epithelial neoplasms. Annu Int Conf IEEE Eng Med Biol Soc 2009:6311-3. https://doi.org/10.1109/IEMBS.2009.5332783

Walsh AJ, Cook RS, Lee JH, Arteaga CL, Skala MC (2015) Collagen density and alignment in responsive and resistant trastuzumab-treated breast cancer xenografts. J Biomed Opt 20:26004. https://doi.org/10.1117/1.JBO.20.2.026004

Watson JM, Marion SL, Rice PF, Bentley DL, Besselsen DG, Utzinger U, Hoyer PB, Barton JK (2014) In vivo time-serial multi-modality optical imaging in a mouse model of ovarian tumorigenesis. Cancer Biol Ther 15:42–60. https://doi.org/10.4161/cbt.26605

Wei SC, Fattet L, Tsai JH, Guo Y, Pai VH, Majeski HE, Chen AC, Sah RL, Taylor SS, Engler AJ, Yang J (2015) Matrix stiffness drives epithelial–mesenchymal transition and tumour metastasis through a TWIST1–G3BP2 mechanotransduction pathway. Nat Cell Biol 17:678–688. https://doi.org/10.1038/ncb3157

Wei X, Li S, He J, Du H, Liu Y, Yu W, Hu H, Han L, Wang C, Li H, Shi X, Zhan M, Lu L, Yuan S, Sun L (2019) Tumor-secreted PAI-1 promotes breast cancer metastasis via the induction of adipocyte-derived collagen remodeling. Cell Commun Signal 17:58. https://doi.org/10.1186/s12964-019-0373-z

Wen B, Campbell KR, Tilbury K, Nadiarnykh O, Brewer MA, Patankar M, Singh V, Eliceiri KW, Campagnola PJ (2016) 3D texture analysis for classification of second harmonic generation images of human ovarian cancer. Sci Rep 6:35734. https://doi.org/10.1038/srep35734

Wen BL, Brewer MA, Nadiarnykh O, Hocker J, Singh V, Mackie TR, Campagnola PJ (2014) Texture analysis applied to second harmonic generation image data for ovarian cancer classification. J Biomed Opt 19:096007. https://doi.org/10.1117/1.JBO.19.9.096007

Williams RM, Zipfel WR, Webb WW (2005) Interpreting second-harmonic generation images of collagen I fibrils. Biophys J 88:1377–1386. https://doi.org/10.1529/biophysj.104.047308

Wu P-C, Hsieh T-Y, Tsai Z-U, Liu T-M (2015) In vivo quantification of the structural changes of collagens in a melanoma microenvironment with second and third harmonic generation microscopy. Sci Rep 5:8879. https://doi.org/10.1038/srep08879

Wu S, Huang Y, Tang Q, Li Z, Horng H, Li J, Wu Z, Chen Y, Li H (2018) Quantitative evaluation of redox ratio and collagen characteristics during breast cancer chemotherapy using two-photon intrinsic imaging. Biomed Opt Express 9:1375–1388. https://doi.org/10.1364/BOE.9.001375

Xia G, Zhi W, Zou Y, Wang L, Wang C, Peng R, Hu X (2017) Non-linear optical imaging and quantitative analysis of the pathological changes in normal and carcinomatous human colorectal muscularis. Pathology 49:627–632. https://doi.org/10.1016/j.pathol.2017.06.002

Xu J, Kang D, Zeng Y, Zhuo S, Zhu X, Jiang L, Chen J, Lin J (2017) Multiphoton microscopy for label-free identification of intramural metastasis in human esophageal squamous cell carcinoma. Biomed Opt Express 8:3360–3368. https://doi.org/10.1364/BOE.8.003360

Xu X, Cheng J, Thrall MJ, Liu Z, Wang X, Wong STC (2013) Multimodal non-linear optical imaging for label-free differentiation of lung cancerous lesions from normal and desmoplastic tissues. Biomed Opt Express 4:2855–2868. https://doi.org/10.1364/BOE.4.002855

Yan J, Zheng Y, Zheng X, Liu Z, Liu W, Chen D, Dong X, Li K, Liu X, Chen G, Lu J, Chen J, Zhuo S, Li G (2016) Real-time optical diagnosis of gastric cancer with serosal invasion using multiphoton imaging. Sci Rep 6:31004. https://doi.org/10.1038/srep31004

Yan J, Zhuo S, Chen G, Milsom JW, Zhang H, Lu J, Zhu W, Xie S, Chen J, Ying M (2014) Real-time optical diagnosis for surgical margin in low rectal cancer using multiphoton microscopy. Surg Endosc 28:36–41. https://doi.org/10.1007/s00464-013-3153-7

Yu X-M, Schneider DF, Leverson G, Chen H, Sippel RS (2013) Follicular variant of papillary thyroid carcinoma is a unique clinical entity: a population-based study of 10,740 cases. Thyroid 23:1263–1268. https://doi.org/10.1089/thy.2012.0453

Yuting L, Li C, Zhou K, Guan G, Appleton PL, Lang S, McGloin D, Huang Z, Nabi G (2018) Microscale characterization of prostate biopsies tissues using optical coherence elastography and second harmonic generation imaging. Lab Invest 98:380–390. https://doi.org/10.1038/labinvest.2017.132

Zeitoune AA, Luna JSJ, Salas KS, Erbes L, Cesar CL, Andrade LALA, Carvalho HF, Bottcher-Luiz F, Casco VH, Adur J (2017) Epithelial ovarian cancer diagnosis of second-harmonic generation images: a semiautomatic collagen fibers quantification protocol. Cancer Inform 16. https://doi.org/10.1177/1176935117690162

Zheng L, Zhuo S, Chen G, Zhu X, Jiang X, Yan J, Chen J, Xie S (2011) Label-free discrimination of normal and fibroadenomal breast tissues using second harmonic generation imaging. Scanning 33:208–210. https://doi.org/10.1002/sca.20234

Zhu GG, Risteli L, Mäkinen M, Risteli J, Kauppila A, Stenbäck F (1995) Immunohistochemical study of type I collagen and type I pN-collagen in benign and malignant ovarian neoplasms. Cancer 75:1010–1017

Zhu H, Chen H, Wang J, Zhou L, Liu S (2019) Collagen stiffness promoted non-muscle-invasive bladder cancer progression to muscle-invasive bladder cancer. Onco Targets Ther 12:3441–3457. https://doi.org/10.2147/OTT.S194568

Zhuo S, Yan J, Chen G, Shi H, Zhu X, Lu J, Chen J, Xie S (2012) Label-free imaging of basement membranes differentiates normal, precancerous, and cancerous colonic tissues by second-harmonic generation microscopy. PLoS One 7: e38655. https://doi.org/10.1371/journal.pone.0038655

Publisher's Note